

Geochemistry of Garga-Sarali intrusive granitoids (central domain of the central African fold belt in Cameroon): petrological implication

**Daama Isaac ¹*, Mbowou Gbambie Isaac Bertrand ², Yamgouot Ngounouno Fadimatou ¹,
Ntounde Mama ², Ngounouno Ismaila ²**

¹ *Department of Earth Sciences, Faculty of Science, University of Ngaoundere, Cameroon*

² *Department of Mineral prospecting and exploration technologies, School of Geology and Mining Engineering*

**Corresponding author E-mail:*

Abstract

The Garga-Sarali granitoids outcrop in form of large slabs and undistorted large blocks, into a schisto-gneissic basement. These rocks contain mainly muscovite and microcline, followed by K-feldspar, quartz, biotite, pyroxene, zircon and oxides, with coarse-grained to fine-grained textures. Geochemical analysis show that it belongs to differentiated rocks group (granodiorite-granite) with high SiO₂ (up to 72 wt%) contents. Their genesis was made from a process of partial melting and fractional crystallization. These rocks are classified as belonging to I- and S-Type, meta-peraluminous, shoshonitic granites; belonging to the domain of volcanic arcs. The rare earth elements patterns suggest a source enriched of incompatible elements. The Nb-Ta and Ti negative anomalies from the multi-element patterns are characteristics of the subduction domains.

Keywords: Geochemistry; Petrology; Granitoids; Shoshonitic; Garga Sarali.

1. Introduction

Garga-Sarali is part of the Adamawa-Yade Orogenesis Domain occurred between 700 and 500 Ma (Fig. 1). During this orogenic period, two kinematic episodes were reported to have controlled the implementation of several generations of Pan- African granitoids (Njanko et al. 2006; Tchameni et al. 2006; Ganwa et al. 2011). The Garga-Sarali granitoids (GSG) outcrop intruded in a schisto-gneissic basement at the South Betare-Oya, a gold mining province. In the studied zone, some lithological surveys of rapid recognition (Gazel and Gerard, 1952; Bessoles and Trompette, 1980; Vairon et al. 1986), partial mapping of field and geophysical works have been formerly carried out. From this previous work, it was found that the Garga-Sarali granitoids have not undergone any geochemistry study (Soba, 1975 ; Ngako et al. 2001). This work aims to present the geochemical data of these rocks in order to identify their petrological origin.

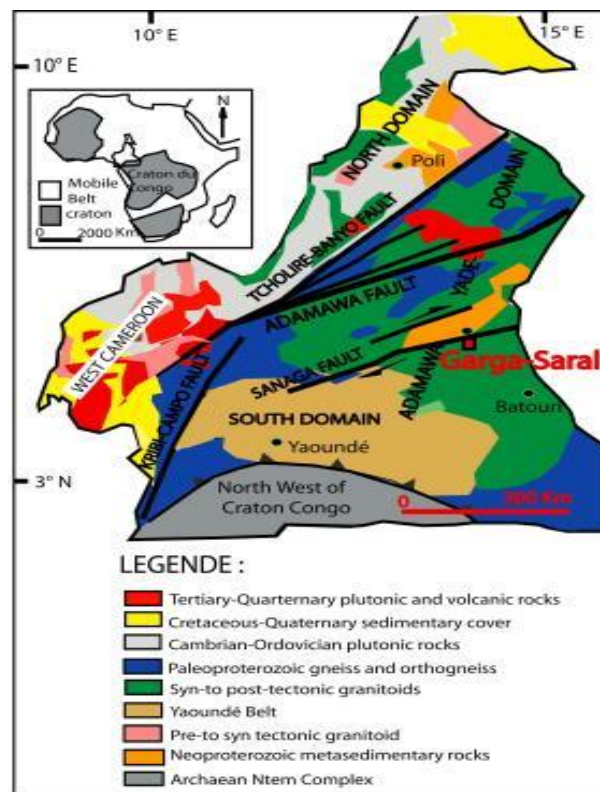


Fig. 1: Geology of Southeastern Cameroon. (A) Geological Map of Cameroon (Modified After [11]). the Inset Is the Map of the African Continent, Showing the Location of Cameroon Relative to the Distribution of Cratons and Mobile Belts. NWC, Northwestern Cameroon Domain; AYD, Adamawa-Yadé Domain; YD, Yaoundé Domain.

2. Geological setting

The central Cameroon domain (Fig. 1) appears as a subset of the Pan-African chain which is highly dominated in the structural point of view by major NE-SW shearing: the Adamawa fault, the Tibati-Banyo fault and the Sanaga Shear zone (Dumont 1986). The Centre-East Cameroon (CEC) is with Toteu et al. (1991) and Toteu et al. (2001): (1) a Paleoproterozoic age set (2100Ma) consisted of granulite metasediments and metaplutonites; (2) a Meso to Neoproterozoic set (1000Ma-700Ma) which includes volcanosedimentary basins, actually distorted and metamorphized into schist (Lom series) and gneiss; and (3) a Pan-african set offset by faults (Nguessi and Vialette, 1994; Tagne-Kamga, 2003) consisted of pre- to syntectonic granitoids including dioritic orthogneiss and calc-alkaline granodiorite (630–620 Ma), syn-tectonic granitoids of S-type granites, porphyroid granites (600–580 Ma) and post-tectonic granitoids represented by alkaline sub-circular masses (550–500 Ma).

3. Methodology and analytical methods

This study is carried out through fieldworks, petrographic description at naked eye and on thin section with polarized microscope. Whole-rock analysis of Garga-Sarali granitoids were done on the representative samples. The analytical methods of ICP-ES and ICP-MS were used at Veritas laboratory in Vancouver, CANADA, to perform a representative analysis of major and trace elements on thirteen samples. The analytical detection limits for major elements are under 0.05 weight % and less than 20 ppm for trace elements.

4. Petrography

Garga-Sarali granitoids (GSG) outcrop as the large slabs (8–50m) and blocks (2–7m). Three petrographic types are identified: the biotite granite (N05°23'33''; E014°01'26''), and the granite with two micas (N05°12'12''; E014°00'08''). (1) The main constituents of biotite granites are quartz, microcline and other feldspars, biotite, Zircon and opaque minerals. Some have a porphyroid texture (western Kongolo granites), medium grained texture (Ndanga-Gadima granite) and others a fine-grained texture (Kongolo granite). These biotite granites are slightly altered and undistorted. (2) Granites with two micas contain quartz, feldspar, muscovite, biotite, pyroxene and oxides. Some enclaves of orthogneiss are intruded in these granitoids. Apart from these rocks, (3) the leucogranites from Petit-Ngaoundere with muscovite are present in the studied zone. These leucogranites are characterized by a fine grain or aplitic texture constituted mainly of muscovite, quartz and feldspar. Some veins of pegmatites and aplites are also present in this area (Fig. 2 and 3).

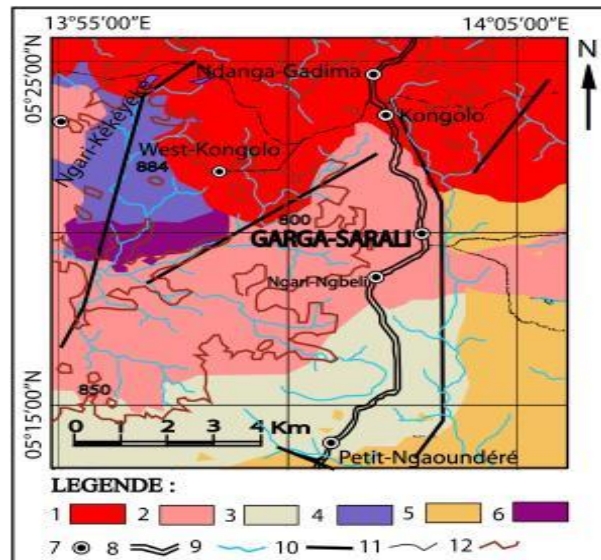


Fig. 2: Sketched Geological Map of Garga-Sarali. 1. Biotite Granite (Ndanga-Gadima, Kongo and West Kongo) 2. Granite with Two Micras from Central Garga-Sarali Zone; 3. Muscovite leucogranite from Petit-Ngaoundéré 4. Schist; 5. Orthogneiss; 6. Migmatite; 7. Locality; 8. Main Road ; 9. Water Bodies ; 10. Fractures; 11. Tracks.

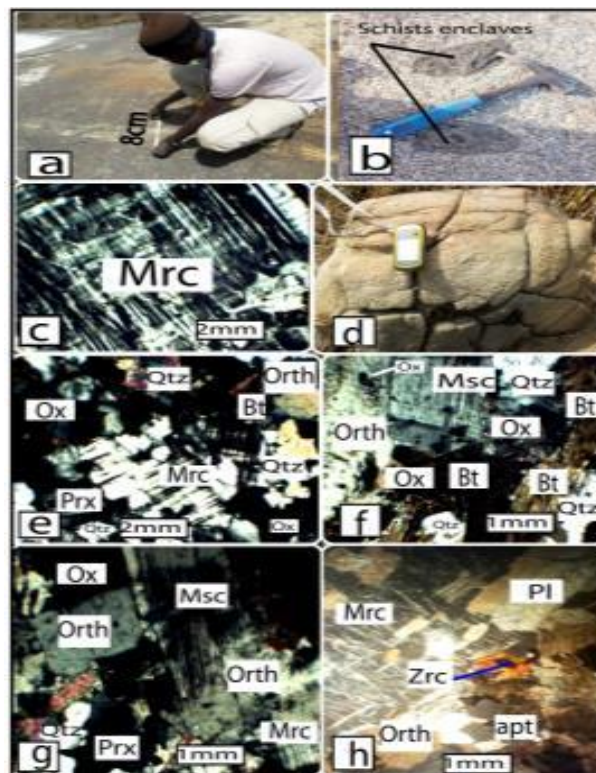


Fig. 3: (A) Muscovite Granite with A Vein of Pegmatite; (B) Enclaves of Schist in the Biotite Granite; (C) Large Microcline Crystals in Thin Section Porphyroid Granite; (D) Block of Biotite Granite with Turtle-Shell ; (F-H) Thin Section of Biotite Granite; (E-H). Thin Section of Granite with Two Micras.

5. Nomenclature and geochemistry data

According to the plutonic rocks classification diagram of (Cox et al. 1979), the studied granitoids are granodiorite for samples from Ndanga-Gadima and West Kongo. Only the data of one sample from West Kongo fall in the granite field (Fig. 4. a). However, all the samples from Kongo, Garga-Sarali Centre and Petit-Ngaoundere are granites. These rocks belong to the shoshonitic domain, excepted two samples from Petit-Ngaoundere and one from Garga-Sarali which fall in to the field of the highly potassic calc-alkaline rocks (Fig. 4. b). SiO_2 contents range from 62.98 wt % to 64.94 wt % for the granodiorite and from 65.13 wt % to 72.72 wt % for the granite (Table 1). Al_2O_3 contents are more or less constant between 14 wt % and 16 wt % for all the studied rocks. The K_2O discrimination in relation to SiO_2 (Fig 4. b) indicates that one sample from West Kongo is alkaline and all others granitoids studied are of sub-alkaline nature.

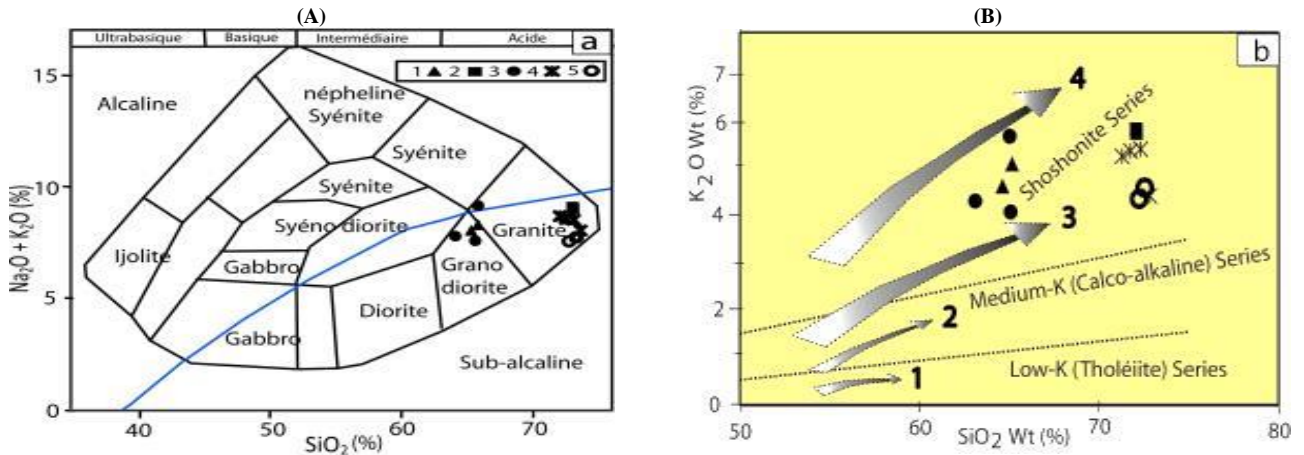


Fig. 4: (A) Plutonic Rocks Classification in the Diagram of (Cox Et Al. 1979) Adapted to Plutonic Rocks by (Wilson 1989). The bold line curve delimits the fields of Alkaline and Sub-Alkaline rocks. This border is from (Irving and Baragar 1971). (B) K_2O vs. SiO_2 Diagram for the classification of potassic domain of the rocks. 1. Ndanga-Gadima biotite granite, 2. Kongolo biotite granite, 3. West Kongolo biotite granite, 4. Granite with two micas from Garga-Sarali Centre, 5. Muscovite leucogranite from Petit-Ngaoundéré.

The Fig. 5 shows that all the biotite granites and granites with two micas of Garga-Sarali Centre belong to the I-type granitoids and leucogranites of Petit-Ngaoundere are from the S-type. The biotite granites of Ndanga-Gadima and West Kongolo are located in the metaluminous field, the biotite granites of Kongolo and the muscovite facies (Garga-Sarali centre and Petit-Ngaoundere) both in metaluminous field. In the Fig. 6 below (Harker, 1909), the Fe_2O_3 , MgO , CaO and Zr contents of the studied Garga-Sarali granitoids decrease. Diagram (Le Maitre, 1989) in Fig. 6 indicates that all Garga-Sarali granitoid types presence a linearly decreasing concentration in the Fe_2O_3 , MgO , CaO and Zr diagram in relation to SiO_2 , and a sub-linearly decreasing concentration in the Al_2O_3 , Ba , Sr and Nb diagram in relation to SiO_2 .

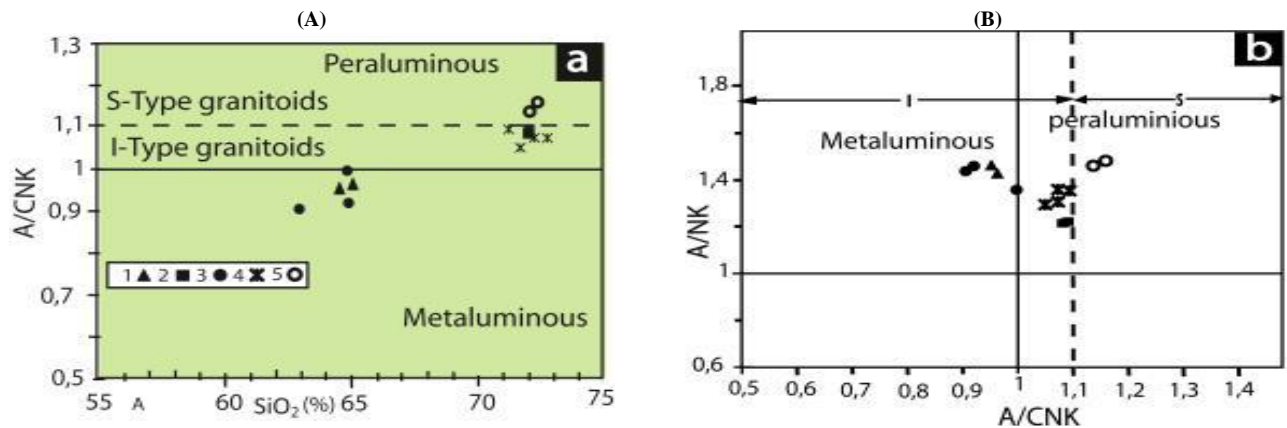


Fig. 5: (A) A/CNK Versus SiO_2 Diagram (After Chappell and White 1992) of the GSG; (B) A/NK Versus A/CNK Diagram (After Shand 1943) For GSG. GSG = Garga-Sarali Granitoids; A = Al_2O_3 ; NK = $Na_2O + K_2O$; CNK = $CaO + Na_2O + K_2O$. 1. Ndanga-Gadima Biotite Granite, 2. Kongolo Biotite Granite, 3. West Kongolo biotite granite, 4. Granite with two micas from Garga-Sarali Centre, 5. Muscovite leucogranite from Petit-Ngaoundéré.

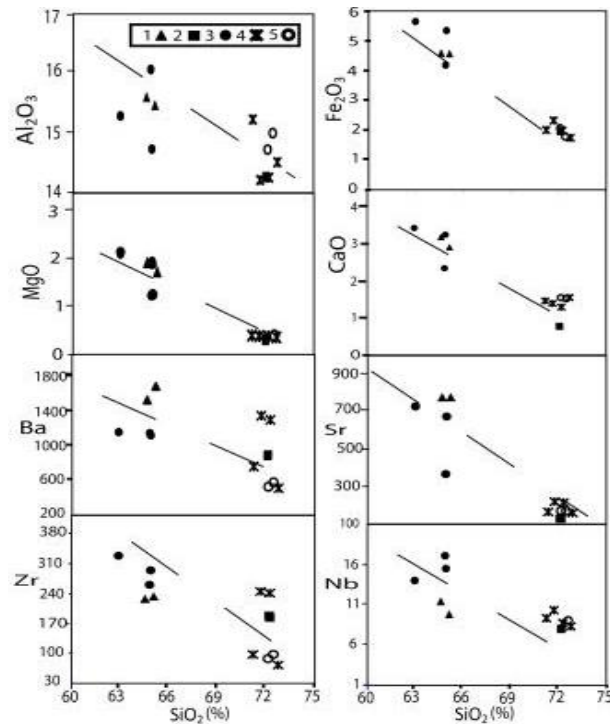


Fig. 6: Al_2O_3 , Fe_2O_3 , MgO , CaO , Ba , Sr , Zr and Nb Diagram in Relation to SiO_2 (Le Maitre 1989) of GSG. GSG = Garga-Sarali Granitoids. 1. Ndanga-Gadima Biotite Granite, 2. Kongolo Biotite Granite, 3. West Kongolo Biotite Granite, 4. Granite with two micas From Garga-Sarali Centre, 5. Muscovite Leucogranite from Petit-Ngaoundéré.

Trace elements data from Garga-Sarali granitoids have been normalized to the primitive mantle (McDonough and Sun, 1995). The REE patterns show a high concentration of light rare earths (LREE) compared to heavy rare earths (HREE) ($(\text{La}/\text{Lu})_N > 1$ and $(\text{La}/\text{Sm})_N > 1$). The Eu negative anomalies are common to all samples and more or less emphasized (Fig. 7, a. and c). The multi-element patterns show a high Large-Ion Lithophile Element (LILE) contents compared to High Field Strength Element (HFSE) contents in these formations. The strong Nb, Ta and Ti negative anomalies characterize all samples of biotite granites, leucogranite and muscovite granites.

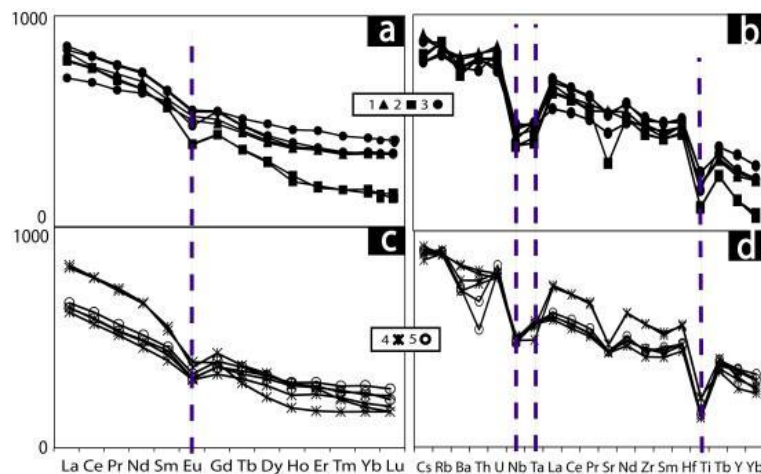


Fig. 7: (A) Rare Earth Elements patterns of Biotite Granites; (B) Multi-Element patterns of Biotite Granites; (C) Rare Earth patterns of Granites with Two Micas and Muscovite Leucogranites; (D) Multi-Element patterns of Granites and Muscovite Leucogranites. All the samples were normalized to the primitive mantle (McDonough and Sun, 1995). 1. Ndanga-Gadima biotite granite, 2. Kongolo biotite granite, 3. West Kongolo biotite granite, 4. Granite with two micas from Garga-Sarali Centre, 5. Muscovite Leucogranite from Petit-Ngaoundéré.

6. Tectonic setting and magmatic protolith nature

According to the Fig. 8 (a and b) all samples fall in the volcanic arc granitoids (VAG) field, which belongs to the subduction zones of magmatic rock as evidenced by Fig. 8 (a, b and c). The molar discrimination of $\text{Al}_2\text{O}_3/(\text{MgO}+\text{FeO})$ in function of $\text{CaO}/(\text{MgO}+\text{FeO})$ (Hoffman et al. 1998) is represented in figure 8.d. This diagram indicates that Kongolo biotite granites are in the partial melting field of metapelites, those of Ndanga-Gadima and West Kongolo fall into the partial melting field of metabasalts and metatonalitics. The granites with two micas of Garga-Sarali Centre and the muscovite leucogranites of Petit-Ngaoundéré are located in the partial melting field of the metagrawacks.

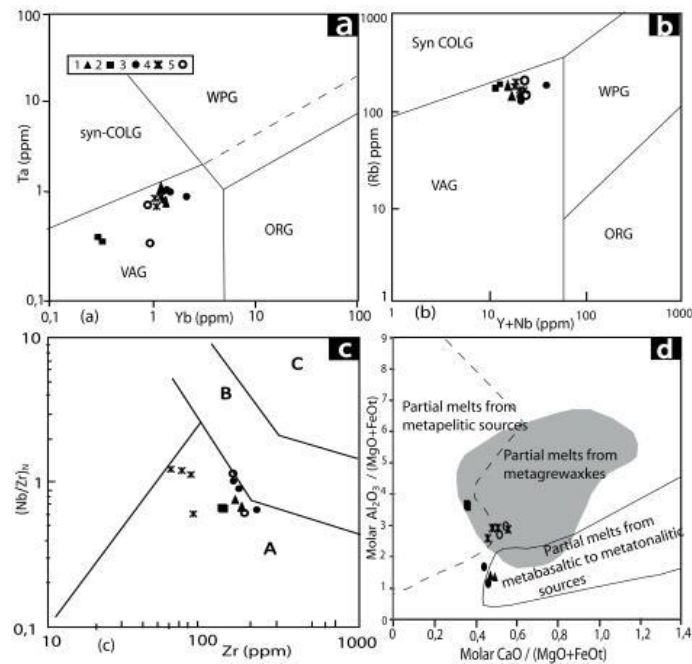


Fig. 8: Tectonic Discrimination Diagram for the Garga-Sarali Granitoids (GSG). Ta vs. Yb (A) and Rb Vs. (Y + Nb) (B) with Discriminative Field After McDonough And Sun (1995): WPG = within Plate Granites; VAG = Volcanic Arc Granites; Syn-COLG = Syn-Collisional Granites; ORG: Oceanic Ridge Granite; (C) Zr Vs. $(Nb/Zr)_h$ Diagram of (Thieblemont and Tegye 1994) for the Studied Granitoids ; (D) Position of the Rocks of Granitoids of Garga-Sarali in the Molar $Al_2O_3/(MgO + FeO)$ - $CaO/(MgO + FeO)$ Diagram (Altherr et al. 2000). Fields of Partial Melts Derived from Experimental Dehydration Melting of Various Source Rocks: (Douce and Beard 1996, Singh and Johannes 1996, Wolf and Wyllie 1994). A = Subduction Zone Magmatic Rocks; B = Collision Zone Rocks; C = Alkaline Intra-Plate Zone Rocks. 1. Ndanga-Gadima Biotite Granite, 2. Kongolo Biotite Granite, 3. West Kongolo Biotite Granite, 4. Granite with Two Micras from Garga-Sarali Centre, 5. Muscovite Leucogranite from Petit-Ngaoundere.

7. Discussions

The granites (Garga-Sarali Centre and Kongolo) are of type I and leucogranites (Petit-Ngaoundere) are of S-type (Fig. 5), but have a hyperaluminous composition ($A/CNK >$) which can justify the fact that they are issued from the partial melting of metapelites and metagrewackes which are of nature rich in aluminum oxide (Altherr et al. 2000 ; Nedelec and Bouchez, 2011). The decreasing linear evolution of all petrographic types in the Al_2O_3 , Fe_2O_3 , MgO, CaO, Ba, Sr Zr and Nb diagrams with respect to SiO_2 (Harker, 1909) would simply reflect their formation by fractional crystallization. All samples fall in the volcanic arc granitoid field, thus highlighting a context of active margin that is more justified by their belonging to the calc-alkaline series. Their high potassic character implies that the arc crust was thicker (Nedelec and Bouchez 2011 ; Barbarin, 1999). The high contents of Al_2O_3 wt% and K_2O wt%, would mainly confirm the abundance of muscovite and microcline in these petrographic types (Fig. 3). The slope ($(La/Lu)_N > 1$ and $(Sm)_N > 1$) (Fig. 7) reveal high contents of Light Rare earth Elements (LREE), this enrichment in incompatible elements is quite evident as they are issued from the crustal melting of stuffy nature in these elements. The Eu negative anomalies common to all samples has to do with its divalent. The correlation of the multi-element spectra of GGS with the granitoids of Tcholliré (Negue et al. 2015), of Meiganga on the Adamawa plateau (Ganwa et al. 2011) and their extension in Central African Republic (Naïmou et al. 2014) is positive. This similarity is based on their positive anomalies in K-Nb-Ta-Ti, which is one more argument to the tectono-magmatism of GGS (Fig. 9). The only significant difference is the behavior of Pb which is slightly positive in these rocks other than GGS. This difference is negligible and not significant, especially since the positive or negative anomaly in Pb is not very determining in the geodynamic context. Its behavior in these other rocks (Meiganga and Tcholliré) can be linked to an effect of magmatic circumstance (impulse of magmatic or hydrothermal fluids, contamination) and sometimes to the initial composition of the magmatic source (Middlemost, 1997). The use of new ICP-MS analysis techniques can simultaneously measure Nb and Ta of GGS with a detection limit of less than 20 ppm, thus improving the accuracy of the Nb / Ta ratio. The average of these ratios barely reaches 11.7 ± 0.6 against 17.5 ± 0.6 of the chondritic ratio considered to be constant (Hoffman et al. 1998; Wedepohl, 1995) (Fig. 9.b). Some have seen in the variations of this Nb/Ta ratio and for the Zr/Hf ratio a manifestation of particular processes such as metasomatism by carbonate fluids (Rudnick et al. 1993). But this argument is antagonistic with the processes having controlled the formations of our GGS.

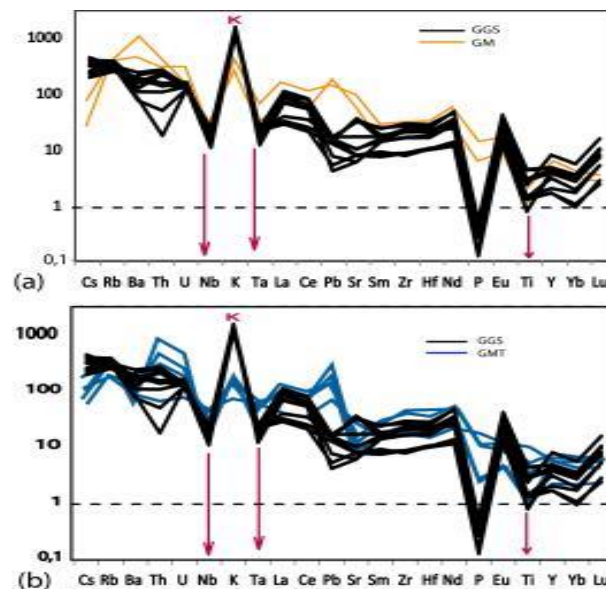


Fig. 9: (A, B). Comparison of the Multi-Element Patterns of the Garga-Sarali Granitoids (GGS) with Those of the Meiganga Granitoids (GM) and Those of the Tcholliré, Meiganga Massif (GMT), Standardized to the Mantle. (C) Nb/Ta as A Function of Zr/Hf of the GGS Compared to the Initial Crust (Bal-louard Et Al. 2016).

8. Conclusion

The study of the Garga-Sarali granitoids permitted us to classify them into three groups: biotite granites (Ndanga-Gadima, Kongolo and West Kongolo), granites with two micas and muscovite leucogranites (Garga-Sarali Centre and Petit-Ngaoundere). They are particularly characterized by their outcrops size and structured texture (fine, medium and coarse grains). They are part of the highly evolved term facies (granodiorites and granites) and are shoshonitic, metaluminous to hyperaluminous. They are mostly issued from the infracrustal melting apart from leucogranites which are of S-type. Metagrewackes, metapelites, metabasalts and metatonalites constitute the main nature of their melted protolith. Both partial melting and fractional crystallization are magmatic processes that are at the origin of their genesis. Their geodynamic context is intimately linked to the subduction of a volcanic island arc lithosphere.

Acknowledgement

Thanks go to the Society of Christian Scholars who financially supported this article project.

References

- [1] Njanko E, Nedelec A, Affaton P (2006) Synkinematic high-K calc-alkaline plutons associated with the Pan-African Central Cameroon shear zone (W-Tibati area): petrology and geodynamic significance. *J Afr Earth Sci.* 44, 494–510. <https://doi.org/10.1016/j.jafrearsci.2005.11.016>.
- [2] Tchameni R., Poulet A, Penaye J, Ganwa AA, Toteu S F (2006) Petrography and geochemistry of the Ngaoundere pan-african granitoids in central north Cameroon: implications for sources and geological setting. *J Afr Earth Sci.* 44 : 511–529. <https://doi.org/10.1016/j.jafrearsci.2005.11.017>.
- [3] Ganwa AA, Siebel W, Frisch W, Shang CK, Ekodeck GE (2011) Geochemistry and Geochronology of the Meiganga Metadiorite: Implications on the Timing of D2 Deformational Phase in Adamawa Yade Domain in Cameroon. *Int J Biol Chem Sci.* 5, 1754–1767. <https://doi.org/10.4314/ijbcs.v5i4.37>.
- [4] Gazel G, Gerard J (1952) Stratigraphie du Précambrien de l'Oubangui Chari Occidental. *Bull Soc Geol Fr* pp 467–483. <https://doi.org/10.2113/gssgfbull.S6-II.7-9.467>.
- [5] Bessoles B., Trompette R (1980) Géologie de l'Afrique : la chaîne panafricaine : « zone mobile – d'Afrique centrale (partie sud) et zone mobile soudanaise ». *Mem Bur Geol Min.* 92, 397.
- [6] Vairon J, Edimo A, Simeon Y, Valda P (1986) protocole d'accord pour la recherche des minéralisations d'or dans la province aurifère de l'Est (Cameroun) Deuxième et troisième phase. 251pp Orleans-France (BRGM).
- [7] Soba D (1975) Le granite intrusif de Nyibi et son auréole de contact (Cameroun). *C R Aca Sci. Fr.* 280, 1935–1938.
- [8] Ngako V, Jegouzo P, Nzenti JP (2001) Le Cisaillement Centre Camerounais Rôle structural et géodynamique dans l'orogénèse panafricaine. *C R Aca Sci. Fr.* 313, 457–463.
- [9] Dumont JF (1986) Identification par télédétection de l'accident de la Sanaga (Cameroun). Sa position dans le contexte des grands accidents d'Afrique Centrale et de la limite nord du craton congolais. *Géodynamique* 1, 13–19.
- [10] Toteu SF, Bertrand JM, Penaye J, Macaudiere J, Angoua S (1991) Cameroon: a tectonic keystone in the Pan-African network. In: LEWRY, J. F. & STAUFFER, M. R. (Eds.): The Early Proterozoic Trans-Hudson Orogeny of North America. *Spec Pap. geol Assoc Canada* 37, 483–496.
- [11] Toteu SF, Van Schmus WR, Penaye J, Michard A (2001) New U-Pb and Sm-Nd Data from north-central Cameroon and its bearing on the pre-pan-African history of central Africa. *Precam Research* 108, 45-73. [https://doi.org/10.1016/S0301-9268\(00\)00149-2](https://doi.org/10.1016/S0301-9268(00)00149-2).
- [12] Nguessi Tchamkam C, Vialette Y (1994) Données géochronologiques (Rb-Sr, Pb-Pb, U-Pb) sur le complexe plutonique de Bandja (Centre-Ouest Cameroun). *C R Acad Sci Paris.*
- [13] Tagne-Kamga G (2003) Petrogenesis of the Neoproterozoic Ngondo plutonic complex (Cameroon, west central Africa): a case of late-collisional ferro-potassic magmatism. *J Afr Earth Scs.* 36, 149–171. [https://doi.org/10.1016/S0899-5362\(03\)00043-5](https://doi.org/10.1016/S0899-5362(03)00043-5).
- [14] Cox KG, Bell JD, Pankhurst RJ (1979) The Interpretation of Igneous Rocks. George, Allen & Unwin, London. 450pp. <https://doi.org/10.1007/978-94-017-3373-1>.
- [15] Harker A (1909) The natural history of igneous rocks. *Nature*, 81, 331–332. <https://doi.org/10.1038/081331a0>.
- [16] McDonough W F, Sun SS, (1995) The Composition of the Earth. *Chem Geol.* 120, 223–253. [https://doi.org/10.1016/0009-2541\(94\)00140-4](https://doi.org/10.1016/0009-2541(94)00140-4).
- [17] Altherr R, Holl A, Hegner E, Langer C, Kreuzer H (2000) High-Potassium Clac-Alkaline I-Type Plutonism in the European Variscides: Northern Vosges (France) and Northern Schwarzwald (Germany). *Lithos* 50, 51–73. [https://doi.org/10.1016/S0024-4937\(99\)00052-3](https://doi.org/10.1016/S0024-4937(99)00052-3).

- [18] Nedelec A, Bouchez JL (2011) *Pétrologie des granites, structure, cadre géologique*. Vuibert Sup STU, 320pp. ISBN : 9782311002867.
- [19] Barbarin B (1999) A Review of the Relationships between Granitoid Types, Their Origins and Their Geodynamic Environments. *Lithos* 46, 605–626. [https://doi.org/10.1016/S0024-4937\(98\)00085-1](https://doi.org/10.1016/S0024-4937(98)00085-1).
- [20] Chappell BW, White AJR (1992) I- and S-Type Granites in the Lachlan Fold Belt. *Transactions of the Royal Society of Edinburgh: Earth Sciences* 83, 1–26. <https://doi.org/10.1017/S0263593300007720>.
- [21] Douce AEP, Beard JS (1996) Effects of P, f(O₂) and Mg/Fe Ratio on Dehydration Melting of Model Metagreywackes. *J Petrol.* 37, 999–1024. <https://doi.org/10.1093/petrology/37.5.999>.
- [22] Le Maitre A (1989) *Classification of Igneous Rocks and Glossary of Terms*. Blackwell Oxford. 193pp.
- [23] Middlemost EAK (1997) *Magma, Rocks, and Planetary Development*. Longman Harlow.
- [24] Negue NE, Tchameni R, Vanderhaeges O, Barbey P, Fosso P (2015) Petrography and Geochemistry of the Mbip Granitic Massif, SW Tchollire (Central North Cameroon): Petrogenetic and Geodynamic Implication. *Int J Geosc.* 6, 761–775. <https://doi.org/10.4236/ijg.2015.67062>.
- [25] Thieblemont D, Tegye M (1994) Une discrimination géochimique des Roches différenciées témoin de la diversité d'origine et de situation Tectonique des magmas calco-alcalins. *C. R. Acad. Sci.*, 319, 87–94.
- [26] Shand SJ (1943) Eruptive rocks: their genesis, composition, classification, and their relations to ore-deposits. *New York* pp : 444.
- [27] Singh J, Johannes W (1996) Dehydration Melting of Tonalites. Part I. Beginning of Melting. *Contrib Mineral Petrol.* 125, 16–25. <https://doi.org/10.1007/s004100050203>.
- [28] Wilson M (1989) *Igneous Petrogenesis. A Global Tectonic Approach*. London, Boston, Sydney, Wellington : Unwin Hyman, xx + 466 pp.
- [29] Irving TN, Baragar WRA (1971) A guide to the chemical classification of the common rocks. *Can. J. Earth Sci.*, 8, 523–548. <https://doi.org/10.1139/e71-055>.
- [30] Wolf MB, Wyllie JP (1994) Deshydration Melting of Amphibolite at 10 Kbar: The Effects of Temperature and Time. *Contrib. Mineral. Petrol.*, 115, 369–383. <https://doi.org/10.1007/BF00320972>.
- [31] Naïmou S, Ganwa AA, Klötzli U, Amadou D, Ekodeck GE (2014) Petrography and Geochemistry of Precambrian Basement Straddling the Cameroon-Chad Border: The Touboro Baïbokoum Area. *Int. J. Geosc.*, 5, 418–431. <https://doi.org/10.4236/ijg.2014.54040>.
- [32] Hoffman PF, Kaufman AJ, Halverson GP, Schrag DP (1998): A Neoproterozoic snowball Earth, *Science*, 281, 1342–1346. <https://doi.org/10.1126/science.281.5381.1342>.
- [33] Wedepohl KH (1995) the composition of the continental crust. *Geochim. Cosmochim. Act.*, 59, 1217–1232. [https://doi.org/10.1016/0016-7037\(95\)00038-2](https://doi.org/10.1016/0016-7037(95)00038-2).
- [34] Rudnick L, McDonough W F, Chappell BW (1993) Carbonatite metasomatism in the northern Tanzania mantle: Petrographic and geochemical characteristics. *Earth planet. Let.*, 114 (4), 463–475. [https://doi.org/10.1016/0012-821X\(93\)90076-L](https://doi.org/10.1016/0012-821X(93)90076-L).
- [35] Ballouard C, Branquet Y, Tartèse R, Poujol M, Boulvais P, Vignerresse J-L (2016) Nb-Ta fractionation in peraluminous granites : A marker of the magmatic-hydrothermal transition : *Geology, Geol. Soc. Amer.*, 44 (7), 395pp. <https://doi.org/10.1130/G38169Y.1>.